J Fluoresc (2016) 26:651–660
DOI 10.1007/s10895-015-1751-6

ORIGINAL ARTICLE

A Fluorescent Switch Sensor for Glutathione Detection Based on Mn-doped CdTe Quantum Dots - Methyl Viologen Nanohybrids

Lurong Yu[1] · **Li Li**[1] · **Yaping Ding**[1] · **Yaxiang Lu**[2]

Received: 18 August 2015 / Accepted: 14 December 2015 / Published online: 16 January 2016

Abstract In the work, a fluorescence switch sensor consists of Mn-doped CdTe quantum dots (QDs) - methyl viologen (MV^{2+}) nanohybrid is fabricated. In the sensor, MV^{2+} plays a role in turning the QDs fluorescence to the "OFF" state due to the efficient electron transfer process while glutathione (GSH) could turn "ON" the native QDs fluorescence by effectively releasing QDs from the QDs-MV^{2+} nanohybrids. In addition, the recovery level of QDs fluorescence is closely related to the amount of GSH. Based on this phenomenon, a reliable and convenient GSH quantitative determination method is established, which not only has a wide determination range of 1.2–200 μM, a low detection limit of 0.06 μM and a short detection time but also can realize the selective detection of GSH upon other competitive biothiols (homocysteine and cysteine) that are coexistent in biological systems. The developed sensor will greatly benefit to the study of GSH amount, helping the understanding of its function in biological systems.

Keywords Mn-doped CdTe · Fluorescence · Switch sensor · Methyl viologen · Glutathione · Determination

✉ Li Li
lilidu@shu.edu.cn

[1] Department of Chemistry, Shanghai University, Shanghai 200444, People's Republic of China

[2] School of Chemical Engineering, University of Birmingham, Birmingham B15 2TT, UK

Introduction

Glutathione (GSH), a bioactive tripeptide (γ-Glu–Cys–Gly) containing sulfhydryl, is the most abundant biothiol in biological systems. It has diversified physiological functions in maintaining the normal operation of biological systems, such as heightening cellular immunity, eliminating free radicals, protecting proteins and other cellular components from oxidation by reactive oxygen species [1–3]. In addition, GSH has a crucial role in holding many cellular functions, like intracellular signal transduction, gene expression, and xenobiotic metabolism [4]. The concentration of GSH in different tissues or organs has a normal level and the abnormal level of GSH may induce to some diseases, such as leukocyte decrease, liver damage, psoriasis, certain cancer, organs aging, cardiopathy, and other ailments [5]. Therefore, the research of convenient and reliable method for the quantitative detection of GSH under physiological conditions is imperative and significant.

To date, various analytical methods have been developed for the detection of GSH, among which capillary zone electrophoresis [6, 7], high performance liquid chromatography [8, 9], electroanalysis [10, 11], spectrophotometry [12, 13], fluorimetry [14, 15] are very typical. Compared with the above-mentioned methods, in recent years, fluorimetry, has been widely used owing to the advantages of simplicity, high sensitivity, specificity and real-time determination. For example, Park et al. used highly fluorescent gold nanoclusters as probes to detect GSH, which relies on blocking Hg^{2+}-induced quenching of the fluorescence of gold nanoclusters that caused by Hg^{2+}-Au^{+} interactions [16]. Zhang et al. realized the detection of GSH based on the polyethyleneimine-capped silver nanoclusters, which could selectively link with GSH and lead to the generation of large non-fluorescent silver nanoparticles [17]. According to the researches, homocysteine (Hcy) and cysteine (Cys) are also

plentifully contained in biological systems, however, most of the reported methods couldn't realize the selective detection of GSH upon Hcy and Cys since these biothiols all incorporate carboxylic, thiol and amino groups, which also could interact with the fluorescence sensor. Therefore, the establishment of methods that can realize the selective detection of GSH upon Hcy and Cys are important. In general, the fluorimetry methods mostly rely on the direct interactions between fluorescent sensors and analytes. However, this detect model usually possesses some defects, such as narrow linear range, high detection limit, low selectivity et al. As an alternative strategy, the fluorescent switch sensor could not only solve this problem to some extent, but also offer a new determination model.

Various materials, such as noble metal nanoparticles [18, 19], fluorescent molecule [20, 21], semiconductor quantum dot (QDs) [22, 23], up-conversion luminescence materials [24], carbon dots [25, 26] and polymers [27] have been widely reported to fabricate fluorescent sensor for the determination of GSH in recent years. Among these reported materials, QDs have attracted considerable attention due to their excellent optical properties, especially for the doped QDs. Compared to the undoped ones, the incorporation of impurities could provide QDs with novel optical properties, including higher fluorescence quantum yield, better photochemical stability, more effective photo-oxidation protection, longer fluorescence lifetime [28], etc. Consequently, doped QDs could act as perfect fluorescence sensor to detect various molecules or ions. For instance, Mn-doped ZnS QDs were used to detect glucose [29], Co^{2+} [30] and sudan dyes [31] and Mn-doped CdTe QDs were employed to determine human IgG [32] and ascorbic acid [33] .

According to what have been discussed above, in the present work, a fluorescent switch sensor for glutathione detection based on Mn-doped CdTe QDs - methyl viologen (MV^{2+}) nanohybrids was fabricated. Water-soluble Mn-doped CdTe QDs were prepared through one-pot synthesis method, by using inorganic salts ($CdCl_2 \cdot 2.5H_2O$ and NaHTe) as precursors and thioglycolic acid (TGA) as the stabilizer. MV^{2+} with two quaternary ammonium groups can link with negatively charged TGA on the surface of QDs through electrostatic interaction. Due to the electron transfer between Mn-doped CdTe QDs and MV^{2+}, the fluorescence intensity of Mn-doped CdTe QDs could be efficiently quenched by MV^{2+}. Nevertheless, the presence of GSH can lead to the recovery of the fluorescence intensity due to the stronger interaction of Cd^{2+}-GSH than that between Cd^{2+} and other thiols or amino acids [34], during which GSH can effectively replace TGA ligands on the surface of Mn-doped CdTe QDs. Therefore, the Mn-doped CdTe QDs fluorescent switch sensor has a high sensitivity and outstanding specificity for GSH detection and can effectively realize the selective detection of GSH upon Hcy and Cys.

Experimental

Materials and Instruments

Ultrapure water was used throughout the experiments. Sodium borohydride ($NaBH_4$, 96 %), tellurium powder (Te, 99.999 %, 100 mesh), cadmium chloride ($CdCl_2 \cdot 2.5H_2O$, analytical purity), manganese chloride ($MnCl_2 \cdot 4H_2O$, analytical purity), thioglycolic acid ($HSCH_2COOH$, analytical purity), methyl viologen ($C_{12}H_{14}Cl_2N_2$, analytical purity), glutathione (GSH, 98 %), and other routine chemicals were of commercial quality, used without further purification. All of the chemicals were purchased from Shanghai Sinopharm Chemical Reagent Co., Ltd. (China). Atomolam tablets were purchased from Guangdong Jianke pharmaceutical Co., Ltd. (China).

Transmission electron microscopy (TEM) images were got using a JEOL-200 CX transmission electron microscope (Japan). OXFORD-INCA energy dispersive spectrometer (EDS) was applied to obtain EDS pattern (Britain). X-ray powder diffraction (XRD) spectra were acquired from a Haoyuan DX-2700 X-ray diffractometer (China). Fourier transform infrared (FTIR) was recorded by an AVATAR 370 Fourier transform infrared spectrophotometer (America). An UV-2501PC spectrometer (Shimadzu, Japan) was adopted to record the ultraviolet visible (UV–vis) absorption spectrum. Via a RF-5301PC spectrofluorophotometer (Shimadzu, Japan), the fluorescence emission spectra were recorded.

Synthesis of TGA-capped Mn-doped CdTe QDs

Firstly, NaHTe precursor solution was prepared according to a previously reported literature [35] with several changes. The molar ratio of Te and $NaBH_4$ was 1 : 20. 2 mmol $NaBH_4$ was dissolved in 6 ml ultrapure water and then degassed with nitrogen flow for 5 min. Subsequently, 0.1 mmol Te was added into the oxygen-free solution. A small outlet linked to the small flask was needed to release the H_2 producing during the reaction. NaHTe solution was obtained by the time the color of solution changed back to colorless and Te was disappeared. The obtained NaHTe solution was used as Te precursor in the following reaction.

Next, the TGA-capped Mn-doped CdTe QDs were prepared relied on a reported research with some modifications [36]. In the current study, the molar ratio of Cd^{2+} / Te^{2-} / TGA was fixed to be 2 : 1 : 4.8 and the Mn^{2+} content was 5 % of cadmium. Briefly, 0.2 mmol $CdCl_2 \cdot 2.5H_2O$ was dissolved in 150 ml ultrapure water. Subsequently, 0.01 mmol $MnCl_2 \cdot 4H_2O$ and 0.48 mmol TGA was injected into the solution. After stirred uniformly, 1 M NaOH solution was adopted and added dropwise into the mixed solution until its pH was adjusted to 7. After that, the dissolved oxygen was driven off by nitrogen flow for about 30 min. Then, the prepared NaHTe

precursor solution was injected quickly into the N_2-saturated solution under vigorous stirring. Immediately, a color change of the solution varied from colorless to orange could be observed distinctly. The Mn-doped CdTe QDs cores were formed during the process. The resulting solution was heated to boil for 10 min under nitrogen protection for the further growth of cores, then transferred it to water bath and reacted at 60 °C for 1 h aimed to obtain Mn-doped CdTe QDs with less surface defects. Finally, the salmon pink TGA-capped Mn-doped CdTe QDs were obtained, and its final concentration was 0.67 mM. After the solution cooled down, storing it in the dark for the further experiments.

XRD, EDS and FTIR Analysis

Same volume of ethanol was added into the prepared TGA-capped Mn-doped CdTe QDs stock solution for the precipitation of QDs, supporting for the further characterization, including EDS, XRD and FTIR analysis.

Measurement of Fluorescence Quantum Yield

The fluorescence emission spectra of the sample solution (TGA-capped Mn-doped CdTe QDs, diluted to 10.72 μM, ultrapure water) and the standard solution (rhodamine B, diluted to 1.2 μM, ultrapure water) were recorded at an excitation wavelength of 350 nm and the slit widths of excitation and emission were both 5 nm (fluorescence spectra throughout the work were all recorded at the measure condition). The fluorescence quantum yield (QY) of TGA-capped Mn-doped CdTe QDs was then calculated according to the following equation:

$$QY_u = QY_S\left(F_u A_s n_u^2\right) \Big/ \left(F_s A_u n_s^2\right) \quad (1)$$

The subscripts "u" and "s" denote sample and standard respectively. "QY" is fluorescence quantum yield. The QY of rhodamine B in water is reported to be 31 %. "A" is absorption values at excitation wavelength. "F" is integrated fluorescence intensity. "n" is the refractive index of solvent.

Detection of GSH

Fluorescent Response of QDs to MV^{2+} Four hundred microliter as-prepared TGA-capped Mn-doped CdTe QDs stock solution and different amounts of 0.03 mM MV^{2+} standard solutions were injected into a series of 25 mL volumetric flasks. Subsequently, diluted the solutions to the marking line with ultrapure water and mixed completely. After the optimal incubation time, the fluorescence spectra of the above solutions were recorded. When the fluorescence intensity of QDs-MV^{2+} system closed to zero, the optimal amount of MV^{2+} serve as the fluorescence "OFF" reagent can be acquired.

Detection of GSH Four hundred microliter TGA-capped Mn-doped CdTe QDs stock solution, an optimal amount of 0.03 mM MV^{2+} standard solution, and different amounts of 0.005 M GSH standard solutions were added into a series of 25 mL volumetric flasks, and then diluted the solutions to the marking line with ultrapure water and mixed thoroughly. After the optimal incubation time, the fluorescence spectra of the above solutions were recorded.

Selectivity Evaluation of the Proposed Method

To evaluate the selectivity of the proposed method to the common amino acids, 400 μL as-prepared QDs stock solution, an optimal amount of 0.03 mM MV^{2+} standard solution, and 1000 μL 0.005 M GSH, Hcy, Cys, alanine (Ala), leucine (Leu), Valine (Val), phenylalanine (Phe), tryptophan (Trp), serine (Ser), lysine (Lys), argnine (Arg), glutamic acid (Glu) standard solutions were injected respectively into a series of 25 mL volumetric flasks, and then diluted the solutions to the marking line with ultrapure water and mixed thoroughly. After the optimal incubation time, the fluorescence spectra of the above solutions were recorded.

To evaluate the effects of some common substances such as NaCl, KI, glucose and glycine on fluorescence response of the reactive systems, two groups of experiments were done. One was about the QDs-MV^{2+} system, 400 μL QDs stock solution, an optimal amount of 0.03 mM MV^{2+} standard solution, and 1000 μL 0.005 M standard solutions of common substances

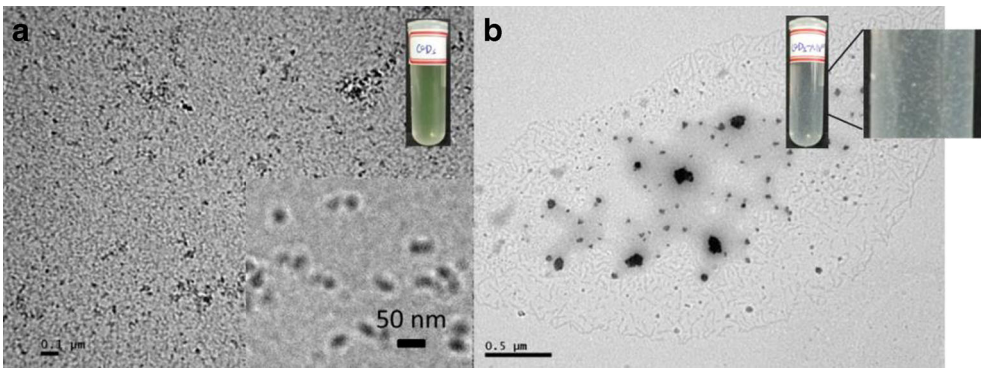

Fig. 1 TEM images of (**a**) TGA-capped Mn-doped CdTe QDs and (**b**) QDs-MV^{2+} nanohybrids. The insets are the dilute solution of QDs and QDs-MV^{2+} nanohybrids, respectively. The QDs-MV^{2+} solution is incubated for 5 days after the addition of MV^{2+}

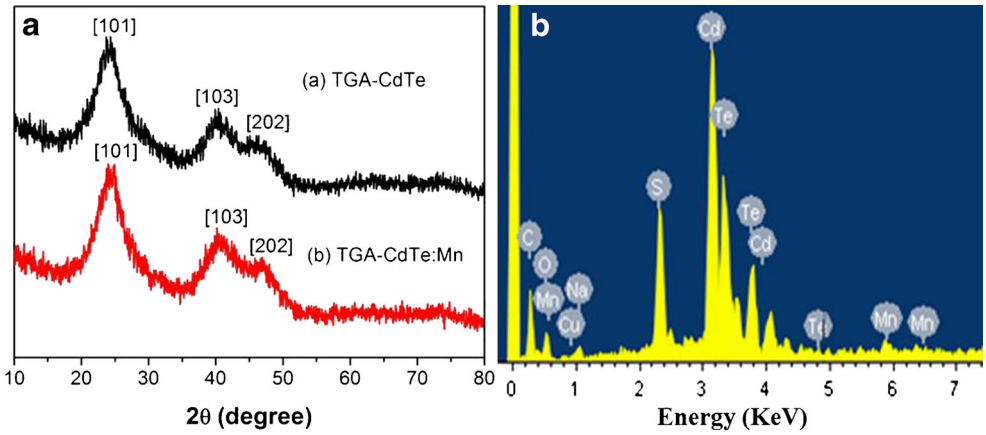

Fig. 2 **a** XRD patterns of TGA-capped CdTe QDs and TGA-capped Mn-doped CdTe QDs, **b** EDS image of TGA-capped Mn-doped CdTe QDs

were added respectively into a series of 25 mL volumetric flasks, and then diluted the solutions to the marking line with ultrapure water and mixed thoroughly. After the optimal incubation time, the fluorescence spectra of the above solutions were recorded. The other was about the QDs-MV^{2+}-GSH system, the protocol was similar with the QDs-MV^{2+} system, the difference was that after the MV^{2+} was added, before the common substances were added, 1000 μL 0.005 M GSH standard solutions were added into the series of 25 mL volumetric flasks. The rest was the same with QDs-MV^{2+} system.

Results and Discussion

Characterization of the as-prepared QDs

Figure 1 displays the typical TEM images of TGA-capped Mn-doped CdTe QDs (Fig. 1a) and QDs-MV^{2+} nanohybrids (Fig. 1b). The insets are the dilute solution of QDs and QDs-MV^{2+} nanohybrids, respectively. The QDs-MV^{2+} solution is incubated for 5 days after the addition of MV^{2+}. From which it can be seen that the as-prepared QDs are spherical in shape, and present good monodisperse with uniform particle sizes about 20 nm. Their dilute solution presents faint yellow and clear. Nevertheless, when the MV^{2+} is added, QDs exhibit spherical aggregates. Five days later, we can observe directly that the aggregation precipitated out from the solution and the color disappeared, which indicated the successful self-assembly between QDs and MV^{2+}.

In order to confirm the structure and elemental composition of the as-prepared QDs, XRD and EDS characterization were performed. Figure 2a shows the powder XRD patterns of TGA-capped Mn-doped CdTe QDs and TGA-capped CdTe QDs. There are three broad and distinct diffractive peaks at 24.35°, 40.62° and 47.12°, which correspond respectively to the crystal planes [101], [103] and [202], confirming that the as-prepared QDs are hexagonal crystalline structure. Compared with the TGA-capped CdTe QDs, the TGA-capped Mn-doped CdTe QDs show no obvious Mn impurity phase, which perhaps attributes to the trace doping of Mn^{2+} that occupied the lattice site and replaced some Cd^{2+}. Figure 2b shows the EDS image of as-prepared QDs, it can be observed that the final product has a strong Cd and Te peaks, and the existence of weak Mn peark also confirmed its trace doping to the CdTe QDs, which is around 2.51 %. Besides, additional signals like carbon, oxygen and sulfur come from the capping agent TGA.

The as-prepared QDs were then analyzed by FT-IR. Figure 3 shows the FT-IR spectra of pure TGA, TGA-capped CdTe QDs, and TGA-capped Mn-doped CdTe QDs. Between the spectra of TGA and QDs, an evident difference can be observed at 2524 cm^{-1}, which belongs to the characteristic absorption of S-H stretching vibration. The disappearance of the S-H band in the two FT-IR spectra of QDs indicates the formation of Cd-S coordination bond, which means the successful conjugation between TGA molecules and QDs.

Usually, UV–vis absorption and fluorescence emission spectrum are applied to describe the optical properties of QDs. As depicts in Fig. 4, the as-prepared TGA-capped Mn-doped CdTe QDs possess a wide UV–vis absorption

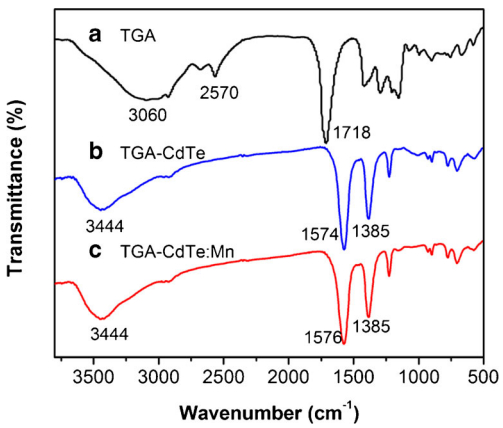

Fig. 3 FT-IR spectra of (**a**) TGA, (**b**) TGA-capped CdTe QDs and (**c**) TGA-capped Mn-doped CdTe QDs

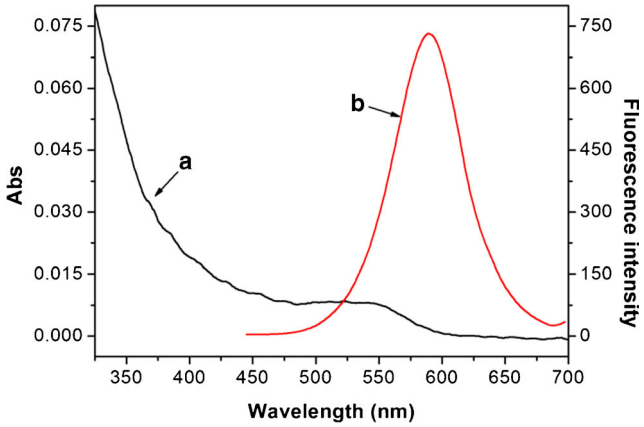

Fig. 4 **a** UV–vis absorption spectrum and **b** fluorescence emission spectrum of TGA-capped Mn-doped CdTe QDs (C_{QDs} = 10.72 μM)

spectrum, indicating the broad absorption wavelength range. Furthermore, a narrow and symmetrical fluorescence emission peak centered at around 575 nm is displayed when the as-prepared QDs are excited by an ultraviolet wavelength of 350 nm. These excellent optical properties of the as-prepared QDs are favorable for their application in the field of analysis. According to the standard expression formula of QY, the calculated QY of TGA-capped Mn-doped CdTe QDs was 36 %.

Optimization of Detection Condition

In order to obtain the optimal detection conditions, the effect of incubation time and the amount of MV^{2+} served as fluorescence "OFF" reagent were investigated in the present study. Figure 5 shows the influence of incubation time on the fluorescence intensity of QDs-MV^{2+} and QDs-MV^{2+}-GSH systems. From the figure we can see that within the initial reaction time for about 8 and 10 min respectively, the fluorescence intensity of the two reaction systems is not stable while it tends to be unchanged after that. Therefore, we choose 8 and 10 min as the optimal incubation time for the two reaction systems, respectively. The effects of different MV^{2+} amounts on the

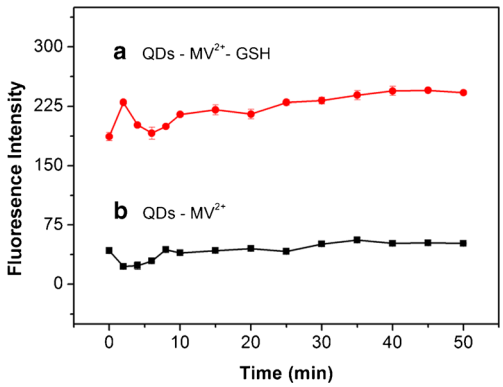

Fig. 5 Effect of incubation time on the fluorescence intensity of **a** QDs-MV^{2+} system and **b** QDs-MV^{2+}-GSH system (C_{QDs} = 10.72 μM, $C_{MV^{2+}}$ = 0.336 μM, C_{GSH} = 0.144 mM)

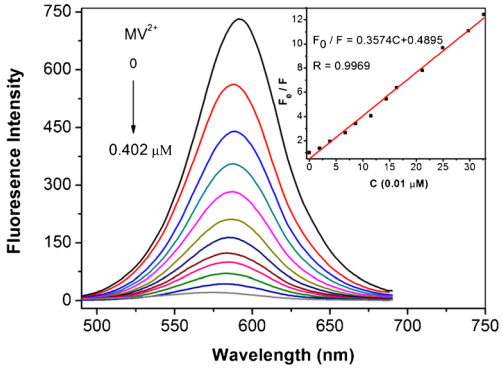

Fig. 6 Fluorescence emission spectra of QDs-MV^{2+} system at different concentrations of MV^{2+} (C_{QDs} = 10.72 μM). The MV^{2+} was added to yield final concentrations of 0, 14, 25, 30, 40, 62, 83, 115, 140, 210, 336, 402 nM. The inset is the calibration curve of relative fluorescence intensity F_0/F versus the concentration of MV^{2+}

fluorescence intensity of TGA-capped Mn-doped CdTe QDs were also conducted and the results are shown in Fig. 6. It is obvious that with the increase of MV^{2+}, the fluorescence intensity of QDs-MV^{2+} system progressively decreased and approached to zero when the amount of MV^{2+} reached to 0.402 μM. Therefore, the optimal amount of MV^{2+} in TGA-capped Mn-doped CdTe QDs solution served as the fluorescence "OFF" reagent was obtained.

Detection of GSH by Restoring the Fluorescence Intensity of TGA-capped Mn-doped CdTe QDs

Figure 7 depicts the fluorescence "OFF-ON" pattern of the established method succinctly. The native fluorescence of the QDs is yellow, after the fluorescence "OFF" reagent MV^{2+} was added, the QDs fluorescence was quenched and the yellow fluorescence disappeared. However, with the

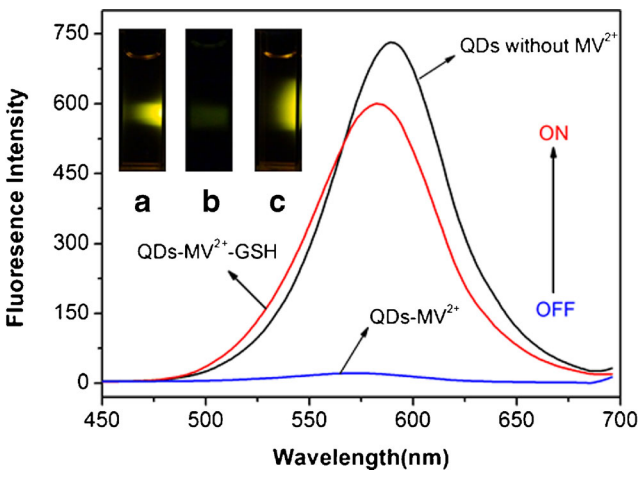

Fig. 7 Fluorescence emission spectra of QDs, QDs-MV^{2+} system and QDs-MV^{2+}-GSH system (C_{QDs} = 10.72 μM, $C_{MV^{2+}}$ = 0.402 μM, C_{GSH} = 0.2 mM). The inset is photographs of (**a**) QDs, (**b**) QDs-MV^{2+} and (**c**) QDs-MV^{2+}-GSH system under 350 nm UV light

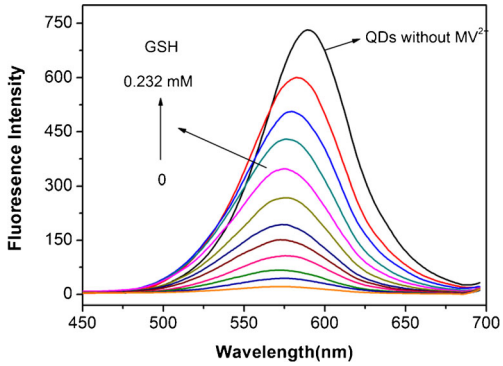

Fig. 8 Fluorescence emission spectra of QDs-MV^{2+}-GSH system at various concentrations of GSH (C_{QDs} = 10.72 μM). The GSH was added to yield final concentrations of 0, 2, 40, 56, 120, 128, 144, 168, 176, 184, 232 μM

addition of fluorescence "ON" reagent GSH, the native fluorescence of the QDs is recovered to some extent.

Under the optimum condition, the detection of GSH based on the change of QDs-MV^{2+} fluorescence intensity was carried out. From Fig. 8 we can see that with the increase of GSH concentration from 0 to 0.232 mM, the fluorescence intensity of QDs-MV^{2+}-GSH system progressively improved, which demonstrates that GSH could act as the fluorescence "on" reagent to restore the fluorescence of QDs. Besides, the fluorescence recovery extent has a close connection with the amount of GSH, based on which a method was developed for the quantitative determination of GSH. A good linear relationship was found between the recovering efficiency (log (F'/F)) and GSH concentration (C) ranges from 1.2 to 200 μM, which can be described by the following equation:

$$log\left(F'/F\right) = 0.0069C + 0.0214(C:\mu M) \quad (2)$$

and the correlation coefficient (R) is 0.9979, as demonstrated in Fig. 9. *F* and *F'* are the fluorescence intensities of QDs-MV^{2+} system and QDs-MV^{2+}-GSH system respectively, and *C* is the concentration of GSH. The detection limit was calculated to be 0.06 μM according to the $3\sigma / k$ criterion, where σ

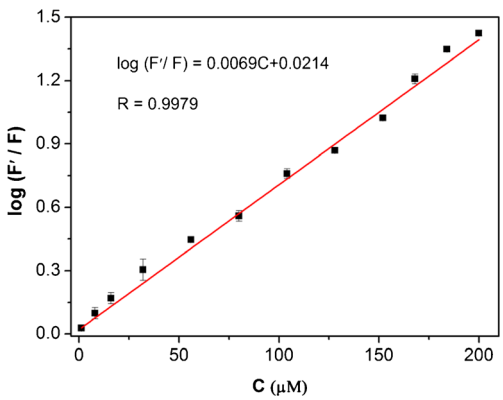

Fig. 9 Calibration curve of the logarithm of relative fluorescence intensity log (F'/F) versus the concentration (C) of GSH

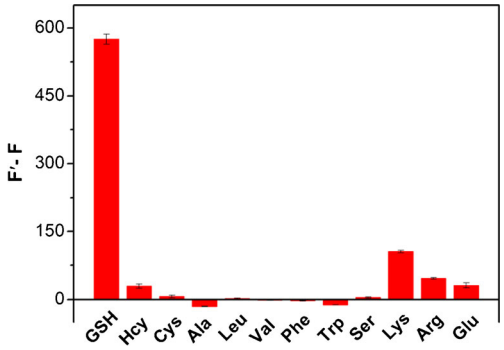

Fig. 10 Fluorescence responses of the QDs-MV^{2+} system to some other common amino acids under identical conditions (the concentrations of the amino acids are 0.2 mM)

is the standard deviation of blank measurements (n = 5) and k is the slope of the calibration curve.

Selectivity Evaluation of the Proposed Method

To evaluate the selectivity of the proposed method for the detection of GSH, the fluorescence responses of the QDs-MV^{2+} system to some similar amino acids under identical conditions were investigated. The result is shown in Fig. 10. It is clealy shown that Lys exhibits a weak turn-on effect on the fluorescence intensity of the QDs-MV^{2+} system while the influence from other amino acids including competitive biothiols such as Hcy, Cys can be negligible. This may be attributed to the two or more potential chelating sites of the GSH (e.g., –SH and –COO) presents to metal ions (e.g., Cd^{2+} and Zn^{2+}). Such chelation makes the interaction of metal ion-GSH stronger than that between metal ion and other amino acids or thiols with single –SH, weak amine or acid chelating sites [34]. Furthermore, the large steric hindrance effect of GSH (larger than Hcy and Cys) always enhances the stability when coordinate with metal ions [37]. Therefore, the established fluorescence switch sensor can realize the selective detection of GSH upon Hcy and Cys under physiological

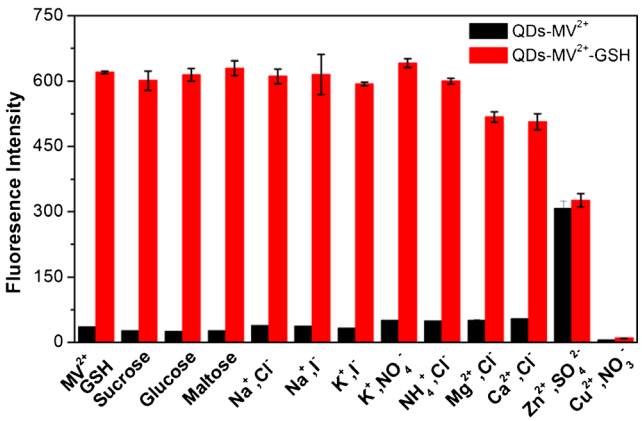

Fig. 11 Effects of saccharides and other common ions on fluorescence response of QDs-MV^{2+} and QDs-MV^{2+}-GSH system

Table 1 Comparison of the optical sensors for the determination of GSH

Probe	Mode	Linear rage	LOD	Detection time	Remark	Rf
AuNPs-Hg^{2+}	Colorimetry	0.025–2.28 μM	17 nM	25 min	Interference from Hcy, Cys	[38]
AuNPs-ppzdtc	Colorimetry	8–250 nM	8 nM	30 min	Difficult synthesis of ppzdtc, time consuming	[39]
MnO_2 NPs-TMB	Colorimetry	0.26–26 μM	0.1 μM	15 min	Interference from Cys	[40]
Fe_3O_4-ABTS-H_2O_2	Colorimetry	3–30 μM	Not giving	20 min	Time consuming	[41]
CQDs-AuNPs	Fluorescence	0.05–3.0 μM	50 nM	5 min	Interference from Hcy, Cys	[42]
Dopamine-CdS:Mn/ZnS QDs	Fluorescence	0–10 mM	Not giving	Not giving	Interference from DTT, complicated operation	[43]
CdSe/ZnS QDs–MV^{2+}	Fluorescence	5–250 μM	0.6 μM	Not giving	Time-consuming	[23]
MnO_2-$NaYF_4$:Yb/Tm NPs	Fluorescence	Not giving	0.9 μM	3 min	Designed for cell imaging	[24]
AuNCs-Hg^{2+}	Fluorescence	0–250 μM	9.4 nM	3 min	Interference from Cys, Hcy	[16]
PEI-AgNCs	Fluorescence	0.5–6 μM	380 nM	30 min	Interference from Cys, Hcy; time consuming	[17]
CdTe QDs-Hg^{2+}	Fluorescence	0.6–20 μM	0.1 μM	10 min	Interference from Cys, Hcy	[37]
g-C_3N_4-Ag^+	Fluorescence	0.02–100 μM	9.6 nM	45 min	Interference from Cys, Hcy; time consuming	[44]
CdTe:Mn QDs-MV^{2+}	Fluorescence	1.2–200 μM	0.06 μM	10 min	–	Present work

conditions. In addition, the effects of some common substances such as NaCl, KI, glucose and glycine on fluorescence response were also investigated and two groups of interference assays were performed. One is the QDs-MV^{2+} system, and the other is QDs-MV^{2+}-GSH system. From the results of interference assays from the two groups, shown in Fig. 11, we can conclude that Mg^{2+}, Ca^{2+} and Zn^{2+} have an unnegligible effect on the fluorescent detection of GSH, and the Cu^{2+} can completely quench the fluorescence of the two reaction systems. Besides, saccharides and other ions like Na^+, K^+, Cl^-,

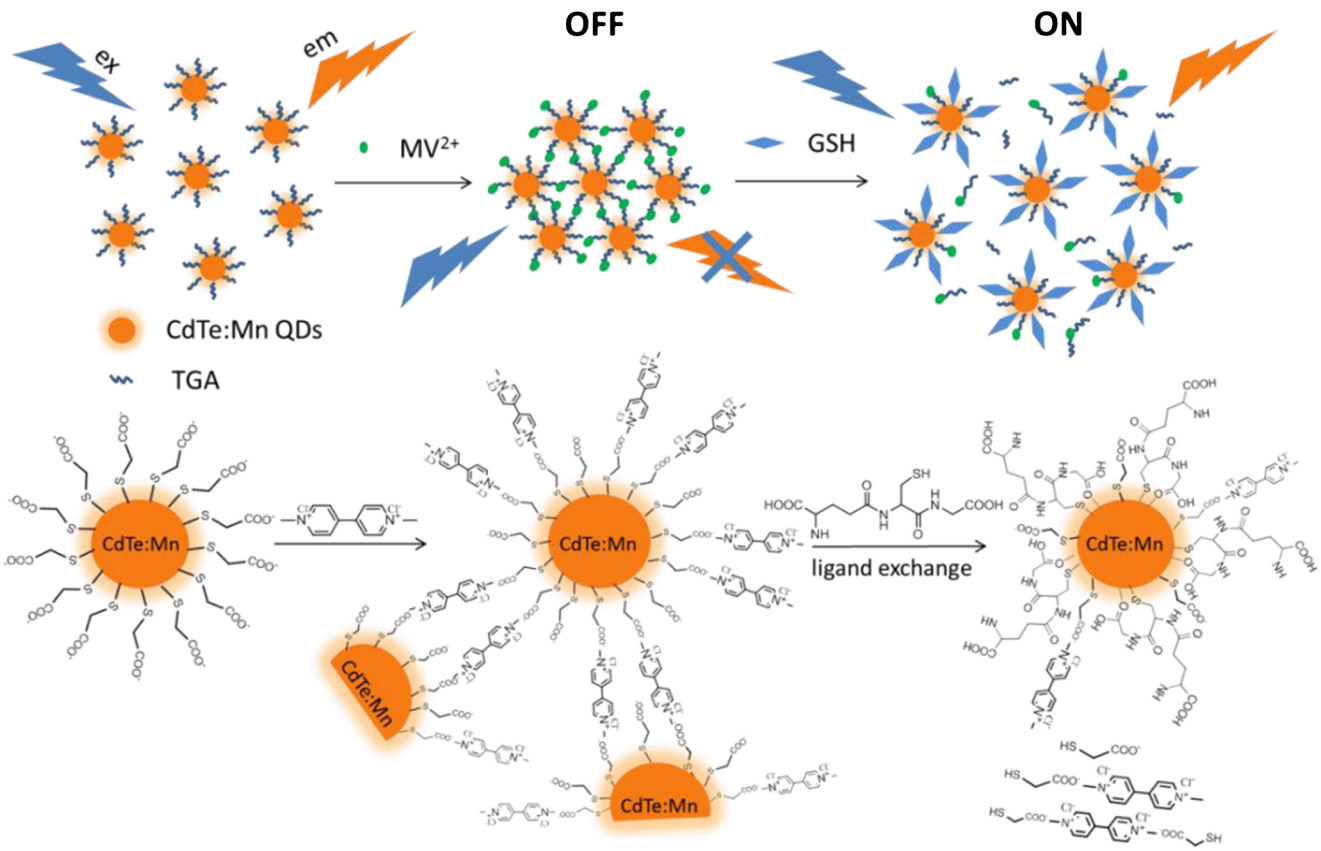

Scheme 1 Current sensing mechanism of the QDs-MV^{2+} "OFF-ON" fluorescent sensor

Table 2 Results of Atomolam tablets sample analysis

Number	Found (μM)	Standard added (μM)	Found after addition (μM)	Average recovery (%)	RSD (%)
1	36.25	20	55.69	97.21	0.87
2	99.56	20	121.08	107.60	3.91
3	99.56	30	131.09	105.11	4.62

NO_3^- have a weak influence in the detection of GSH. Consequently, we can conclude that the established fluorescence switch sensor has a higher selectivity.

Comparison with Other Optical Sensors

Compared with other optical sensors reported to detect GSH in recent years, the fabricated Mn-doped CdTe QDs - MV^{2+} sensor has advantages in the highly selective detection of GSH in the presence of Hcy and Cys, the short incubation time, the wider linear range and the real-time detection. The results are shown in Table 1.

The Possible Sensing Mechanism

Scheme 1 depicts the mechanism of the "OFF-ON" QDs-MV^{2+} fluorescent sensor in the detection of GSH. When MV^{2+} with two quaternary ammonium groups was added to the as-prepared QDs solution, it will link with negatively charged TGA on the surface of QDs through electrostatic interaction. Therefore, MV^{2+} can serve as the linkers between individual QDs, which combined the independent QDs together and enabled them to form spherical QDs-MV^{2+} nanohybrids spontaneously. The attached MV^{2+}, as a strong electron transfer agent, caused the fluorescence of QDs in the "OFF" state through an efficient electron transfer process [45]. Nevertheless, the subsequent addition of GSH could effectively displaced a large proportion of TGA ligands and then make the QDs release from the QDs-MV^{2+} nanohybrids. Consequently, the electron transfer process between QDs and MV^{2+} couldn't occur anymore, which restored the native fluorescence of the QDs to the "ON" state.

Analytical Application

To verify the practical feasibility of the proposed sensor in clinical applications, the Mn-doped CdTe QDs-MV^{2+} nanohybrids were utilized for GSH detection in commercial Atomolam tablets. The average recovery and relative standard deviation (RSD) were obtained according to the standard addition method. As shown in Table 2, an average recovery of 97.21 to 107.60 % was acquired. Moreover, the relative standard deviation (RSD) was lower than 5 %, which indicated a precision of this method that can meet the requirements of microanalysis. Therefore, the developed method is feasible to the determination of GSH.

Conclusions

In the present work, a facile strategy was adopted to fabricate the QDs-MV^{2+} nanohybrids, based on which a novel and convenient fluorescence switch sensor was successfully established for the quantitative detection of GSH. Water-soluble TGA-capped Mn-doped CdTe QDs with excellent optical properties were prepared through one-pot synthesis method. The fluorescence restoring of QDs is closely related to the amount of GSH, a good linear relationship between the fluorescence intensity of the QDs-MV^{2+} system and the concentration of GSH in the range of 1.2 to 200 μM could be achieved. This sensor not only can effectively detect GSH with high sensitivity, but also shows high selectivity over other related thiols (Hcy or Cys) and amino acids. The developed sensor will greatly benefit to the study of GSH level, helping to understand its function in biological systems.

Acknowledgments This research is supported by the National Natural Science Foundation of China (NSFC) (No. 21271127, 61171033), the Nano-Foundation of Science and Techniques Commission of Shanghai Municipality (No. 12nm0504200) and the Natural Science Foundation of Shanghai Municipality (No. 13ZR1415600).

References

1. Atli G, Canli M (2008) Responses of metallothionein and reduced glutathione in a freshwater fish Oreochromis niloticus following metal exposures. Environ Toxicol Pharmacol 25:33–38. doi:10.1016/j.etap.2007.08.007
2. Yin J, Kwon Y, Kim D, Lee D, Kim G, Hu Y, Ryu JH, Yoon J (2014) Cyanine-based fluorescent probe for highly selective detection of glutathione in cell cultures and live mouse tissues. J Am Chem Soc 136:5351–5358. doi:10.1021/Ja412628z
3. Yuan Y, Zhang J, Wang MJ, Mei B, Guan YF, Liang GL (2013) Detection of glutathione in vitro and in cells by the controlled self-assembly of nanorings. Anal Chem 85:1280–1284. doi:10.1021/Ac303183v
4. Krauth-Siegel RL, Bauer H, Schirmer H (2005) Dithiol proteins as guardians of the intracellular redox milieu in parasites: old and new drug targets in trypanosomes and malaria-causing plasmodia. Angew Chem Int Ed 44:690–715. doi:10.1002/anie.200300639

5. Lu SC (2009) Regulation of glutathione synthesis. Mol Aspects Med 30:42–59. doi:10.1016/j.mam.2008.05.005
6. Hodakova J, Preisler J, Foret F, Kuban P (2015) Sensitive determination of glutathione in biological samples by capillary electrophoresis with green (515 nm) laser-induced fluorescence detection. J Chromatogr A 1391:102–108. doi:10.1016/j.chroma.2015.02.062
7. Shen CC, Tseng WL, Hsieh MM (2012) Selective extraction of thiol-containing peptides in seawater using Tween 20-capped gold nanoparticles followed by capillary electrophoresis with laser-induced fluorescence. J Chromatogr A 1220:162–168. doi:10.1016/j.chroma.2011.11.057
8. Kominkova M, Horky P, Cernei N, Tmejova K, Ruttkay-Nedecky B, Guran R, Pohanka M, Zitka O, Adam V, Kizek R (2015) Optimization of the glutathione detection by high performance liquid chromatography with electrochemical detection in the brain and liver of rats fed with taurine. Int J Electrochem Sci 10:1716–1727
9. Bayram B, Runbach G, Frank J, Esatbeyoglu T (2014) Rapid method for glutathione quantitation using high-performance liquid chromatography with coulometric electrochemical detection. J Agric Food Chem 62:402–408. doi:10.1021/Jf403857h
10. Rezaei B, Khosropour H, Ensafi AA, Hadadzadeh H, Farrokhpour H (2015) A differential pulse voltammetric sensor for determination of glutathione in real samples using a Trichloro(terpyridine) ruthenium (III)/Multiwall carbon nanotubes modified paste electrode. IEEE Sens J 15:483–490. doi:10.1109/Jsen.2014.2343152
11. Yuan BQ, Zhang RC, Jiao XX, Li J, Shi HZ, Zhang DJ (2014) Amperometric determination of reduced glutathione with a new Co-based metal-organic coordination polymer modified electrode. Electrochem Commun 40:92–95. doi:10.1016/j.elecom.2014.01.006
12. Ni PJ, Sun YJ, Dai HC, Hu JT, Jiang S, Wang YL, Li Z (2015) Highly sensitive and selective colorimetric detection of glutathione based on Ag [I] ion-3,3 ′,5,5 ′-tetramethylbenzidine (TMB). Biosens Bioelectron 63:47–52. doi:10.1016/j.bios.2014.07.021
13. Chen ZG, Wang Z, Chen JH, Wang SB, Huang XP (2012) Sensitive and selective detection of glutathione based on resonance light scattering using sensitive gold nanoparticles as colorimetric probes. Analyst 137:3132–3137. doi:10.1039/C2an35405e
14. Hu ZQ, Sun LL, Gu YY, Jiang Y (2015) A sensitive and selective fluorescent probe for detection of glutathione in the presence of Cu2+ and its application to biological imaging. Sensors Actuators B Chem 212:220–224. doi:10.1016/j.snb.2015.01.084
15. Hou XF, Guo XL, Chen B, Liu CH, Gao F, Zhao J, Wang JH (2015) Rhodamine-based fluorescent probe for highly selective detection of glutathione over cysteine and homocysteine. Sensors Actuators B Chem 209:838–845. doi:10.1016/j.snb.2014.12.009
16. Park KS, Kim MI, Woo MA, Park HG (2013) A label-free method for detecting biological thiols based on blocking of Hg2+ −quenching of fluorescent gold nanoclusters. Biosens Bioelectron 45:65–69. doi:10.1016/j.bios.2013.01.047
17. Zhang N, Qu F, Luo HQ, Li NB (2013) Sensitive and selective detection of biothiols based on target-induced agglomeration of silver nanoclusters. Biosens Bioelectron 42:214–218. doi:10.1016/j.bios.2012.10.090
18. Guan ZP, Li S, Cheng PBS, Zhou N, Gao NY, Xu QH (2012) Band-selective coupling-induced enhancement of two-photon photoluminescence in gold nanocubes and its application as turn-on fluorescent probes for cysteine and glutathione. ACS Appl Mater Interfaces 4:5711–5716. doi:10.1021/Am301822v
19. Liu XD, Sun R, Ge JF, Xu YJ, Xu Y, Lu JM (2013) A squaraine-based red emission off-on chemosensor for biothiols and its application in living cells imaging. Org Biomol Chem 11:4258–4264. doi:10.1039/C3ob40502h
20. Guo YS, Wang H, Sun YS, Qu B (2012) A disulfide bound-molecular beacon as a fluorescent probe for the detection of reduced glutathione and its application in cells. Chem Commun 48:3221–3223. doi:10.1039/C2cc17552e
21. Isik M, Ozdemir T, Turan IS, Kolemen S, Akkaya EU (2013) Chromogenic and fluorogenic sensing of biological thiols in aqueous solutions using BODIPY-based reagents. Org Lett 15:216–219. doi:10.1021/Ol303306s
22. Xu Q, Wei HP, Hu XY (2013) Glutathione detection based on ZnS quantum-dot-based OFF-ON fluorescent probe. Chin J Anal Chem 41:1102–1106. doi:10.3724/Sp.J.1096.2013.21154
23. Liu JF, Bao CY, Zhong XH, Zhao CC, Zhu LY (2010) Highly selective detection of glutathione using a quantum-dot-based OFF-ON fluorescent probe. Chem Commun 46:2971–2973. doi:10.1039/B924299f
24. Deng RR, Xie XJ, Vendrell M, Chang YT, Liu XG (2011) Intracellular glutathione detection using MnO2-Nanosheet-Modified upconversion nanoparticles. J Am Chem Soc 133:20168–20171. doi:10.1021/Ja2100774
25. Zhou L, Lin YH, Huang ZZ, Ren JS, Qu XG (2012) Carbon nanodots as fluorescence probes for rapid, sensitive, and label-free detection of Hg2+ and biothiols in complex matrices. Chem Commun 48:1147–1149. doi:10.1039/C2cc16791c
26. Ran X, Sun HJ, Pu F, Ren JS, Qu XG (2013) Ag Nanoparticle-decorated graphene quantum dots for label-free, rapid and sensitive detection of Ag+ and biothiols. Chem Commun 49:1079–1081. doi:10.1039/C2cc38403e
27. Huang H, Shi FP, Li YA, Niu L, Gao Y, Shah SM, Su XG (2013) Water-soluble conjugated polymer-Cu(II) system as a turn-on fluorescence probe for label-free detection of glutathione and cysteine in biological fluids. Sensors Actuators B Chem 178:532–540. doi:10.1016/j.snb.2013.01.003
28. Pradhan N, Peng XG (2007) Efficient and color-tunable Mn-doped ZnSe nanocrystal emitters: control of optical performance via greener synthetic chemistry. J Am Chem Soc 129:3339–3347. doi:10.1021/Ja068360v
29. Sharma M, Jain T, Singh S, Pandey OP (2012) Tunable emission in surface passivated Mn-ZnS nanophosphors and its application for Glucose sensing. Aip Adv 2. doi: 10.1063/1.3698310
30. Bian W, Ma J, Liu QL, Wei YL, Li YF, Dong C, Shuang SM (2014) A novel phosphorescence sensor for Co2+ ion based on Mn-doped ZnS quantum dots. Luminescence 29:151–157. doi:10.1002/Bio.2520
31. Zhou M, Chen XF, Xu YY, Qu JC, Jiao LX, Zhang HG, Chen HL, Chen XG (2013) Sensitive determination of Sudan dyes in foodstuffs by Mn-ZnS quantum dots. Dyes Pigments 99:120–126. doi:10.1016/j.dyepig.2013.04.027
32. Liang GX, Pan HC, Li Y, Jiang LP, Zhang JR, Zhu JJ (2009) Near infrared sensing based on fluorescence resonance energy transfer between Mn:CdTe quantum dots and Au nanorods. Biosens Bioelectron 24:3693–3697. doi:10.1016/j.bios.2009.05.008
33. Li L, Cai XY, Ding YP, Gu SQ, Zhang QL (2013) Synthesis of Mn-doped CdTe quantum dots and their application as a fluorescence probe for ascorbic acid determination. Anal Methods 5:6748–6754. doi:10.1039/C3ay41257a
34. DiazCruz MS, Mendieta J, Tauler R, Esteban M (1997) Cadmium-binding properties of glutathione: a chemometrical analysis of voltammetric data. J Inorg Biochem 66:29–36. doi:10.1016/S0162-0134(96)00156-0
35. Zhang YH, Zhang HS, Ma M, Guo XF, Wang H (2009) The influence of ligands on the preparation and optical properties of water-soluble CdTe quantum dots. Appl Surf Sci 255:4747–4753. doi:10.1016/j.apsusc.2008.09.009
36. Zhang LJ, Xu CL, Li BX (2009) Simple and sensitive detection method for chromium(VI) in water using glutathione-capped CdTe quantum dots as fluorescent probes. Microchim Acta 166:61–68. doi:10.1007/s00604-009-0164-0

37. Han BY, Yuan JP, Wang EK (2009) Sensitive and selective sensor for biothiols in the cell based on the recovered fluorescence of the CdTe quantum dots-Hg(II) system. Anal Chem 81:5569–5573. doi:10.1021/Ac900769h
38. Xu H, Wang YW, Huang XM, Li Y, Zhang H, Zhong XH (2012) Hg2+—mediated aggregation of gold nanoparticles for colorimetric screening of biothiols. Analyst 137:924–931. doi:10.1039/C2an15926k
39. Li Y, Wu P, Xu H, Zhang H, Zhong XH (2011) Anti-aggregation of gold nanoparticle-based colorimetric sensor for glutathione with excellent selectivity and sensitivity. Analyst 136:196–200. doi:10.1039/C0an00452a
40. Liu X, Wang Q, Zhang Y, Zhang LC, Su YY, Lv Y (2013) Colorimetric detection of glutathione in human blood serum based on the reduction of oxidized TMB. New J Chem 37:2174–2178. doi:10.1039/C3nj40897c
41. Ma YH, Zhang ZY, Ren CL, Liu GY, Chen XG (2012) A novel colorimetric determination of reduced glutathione in A549 cells based on Fe3O4 magnetic nanoparticles as peroxidase mimetics. Analyst 137:485–489. doi:10.1039/C1an15718c
42. Shi YP, Pan Y, Zhang H, Zhang ZM, Li MJ, Yi CQ, Yang MS (2014) A dual-mode nanosensor based on carbon quantum dots and gold nanoparticles for discriminative detection of glutathione in human plasma. Biosens Bioelectron 56:39–45. doi:10.1016/j.bios.2013.12.038
43. Banerjee S, Kar S, Perez JM, Santra S (2009) Quantum dot-based OFF/ON probe for detection of glutathione. J Phys Chem C 113:9659–9663. doi:10.1021/Jp9019574
44. Tang YR, Song HJ, Su YY, Lv Y (2013) Turn-on persistent luminescence probe based on graphitic carbon nitride for imaging detection of biothiols in biological fluids. Anal Chem 85:11876–11884. doi:10.1021/Ac403517u
45. Matylitsky VV, Dworak L, Breus VV, Basche T, Wachtveitl J (2009) Ultrafast charge separation in multiexcited CdSe quantum dots mediated by adsorbed electron acceptors. J Am Chem Soc 131:2424. doi:10.1021/Ja808084y